Diffraction Shaders

Jos Stam*

Alias | wavefront

Abstract

The reflection of light from surfaces is a fundamental problem in computer graphics. Although many reflection models have been proposed, few take into account the wave nature of light. In this paper, we derive a new class of reflection models for metallic surfaces that handle the effects of diffraction. Diffraction is a purely wave-like phenomenon and cannot be properly modeled using the ray theory of light alone. A common example of a surface which exhibits diffraction is the compact disk. A characteristic of such surfaces is that they reflect light in a very colorful manner. Our model is also a generalization of most reflection models encountered in computer graphics. In particular, we extend the He-Torrance model to handle anisotropic reflections. This is achieved by rederiving, in a more general setting, results from surface wave physics which were taken for granted by other researchers. Specifically, our use of Fourier analysis has enabled us to tackle the difficult task of analytically computing the Kirchhoff integral of surface scattering.

CR Categories: I.3.7 [Computer Graphics]: Three-Dimensional Graphics and Realism—Color, shading, shadowing, and texture J.2 [Physical Sciences and Engineering]: Physics

Keywords: shading models, diffraction, Fourier transform, Kirchhoff theory, rough surface scattering, random processes

1 Introduction

The modeling of the interaction of light with surfaces is one of the main goals of computer graphics. Over the last thirty years many reflection models have been proposed that have considerably improved the quality of computer graphics imagery. Almost all of these reflection models are either empirical or based on the ray theory of light. Surprisingly little attention has been devoted to the purely wave-like character of light. It is well known from physical optics that ray theory is only an approximation of the more fundamental wave theory. Why then has wave theory been so neglected ? The main reason is that the ray theory is sufficient to visually capture the reflected field from many commonly occurring surfaces. This observation is usually true when the surface detail is much larger than the wavelength of visible light (roughly 0.5 microns (10^{-6} meters)). Another reason for this neglect is the common belief that models based on wave theory are computationally too expensive to be of any use in computer graphics. In this paper we challenge this point of view by introducing a new class of analytical reflection models which simulate the effects of *diffraction*. Diffraction is a purely wave-like phenomenon which cannot be modeled using the standard ray theory of light. Diffraction occurs when the surface detail is comparable to the wavelength of light. A common example of a surface that produces visible diffraction patterns is the compact disk (CD). By rotating a CD under a steady light source, one can fully appreciate the visual complexity of diffraction. To capture these subtle changes in color and intensity requires a wave-like description of light. In this paper we derive analytical reflection models based on the wave theory that capture the effects of diffraction. In addition, our model is both easy to implement as a standard "shader" and computationally efficient. The derivation which leads to our new model, however, is not simple. This is because the wave theory is mathematically much more complex than the ray theory of light.

Scanning through the computer graphics literature, we found only a few references which explicitly use the wave description of light. In 1981 Moravec proposed solving the global illumination problem using the wave theory of light [11]. For his method to give acceptable results, both a very fine resolution (on the order of the wavelength of light) and a large ensemble of simulations (to model incoherent natural light sources) are required. This makes his approach unsuitable for practical computer graphics applications. Later in 1985, Kajiya proposed to numerically solve the Kirchhoff integral[1] to simulate the light reflected from anisotropic surfaces [9]. His approach, although less ambitious than Moravec's, suffers from the same limitations. In this context it would appear to be more promising to solve directly for the coherence functions associated with the waves, which are second order statistical averages of the wave fields. Some work in this area has been pursued by Tannenbaum et al. [20]. The coherence functions can also be employed to define generalized radiances [23].

A more practical use of the wave theory in computer graphics is to employ it to derive analytical reflection models. This approach, which has a long history in the applied optics literature, e.g., [2], was first seriously introduced to computer graphics by Bahar and Chakrabarti [1]. Using Bahar's full wave theory, they were able to fit analytical distributions to their computations for surfaces having a large isotropic surface roughness. The full wave theory has the advantage over the Kirchhoff theory in that it takes into account the global shape of the object. However, in practice analytical expressions are known only for simple objects such as spheres. Also the *global* shapes of surfaces in computer graphical models are usually much larger than the wavelength of light. Later in 1991, He and collaborators derived a general reflection model based on the electro-magnetic wave theory to predict the reflection of light from isotropic surfaces of any surface roughness [8]. At about the same time, a very similar model was proposed in the computer vision literature by Nayar [13]. As in Kajiya's work, these two models are essentially based on the Kirchhoff approximation of surface reflection [2]. We also note that Blinn already used some asymptotic results from Beckmann's monograph [3]. However, Blinn's model does not account for wave-like effects.

*Alias | wavefront, 1218 Third Ave, 8th Floor, Seattle, WA 98101, U.S.A. jstam@aw.sgi.com

[1] This integral will be defined more precisely below.

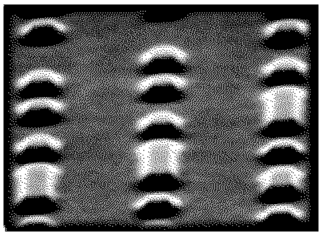

Figure 1: Close-up "view" of the micro-geometry of the surface of a compact disk.

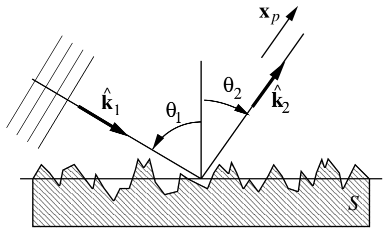

Figure 2: Basic geometry of the surface wave reflection problem.

Although the analytical models just discussed are based on wave theory, none of them is able to capture the visual complexity of the light reflected off of a compact disk, for example. The main reason is that these models assume the surface detail to be isotropic, i.e., the surface "looks the same" in every direction. Interesting diffraction phenomena, however, occur mostly when the surface detail is highly *anisotropic*, viz. non-isotropic. Fig. 1 shows that this is certainly the case for the CD. Other examples include brushed metals and colorful diffraction gratings. In computer graphics, both empirical and ray optics models have been proposed to model the reflection from anisotropic surfaces [15, 17, 22]. However, since these models are not based on wave theory, they failed to capture the effects of diffraction. To the best of our knowledge, reflection models that handle colorful diffraction effects have not appeared in the computer graphics literature or in any commercially available graphics software before. The phenomenon of diffraction was used, however, by Nakamae et al. to model the fringes caused when viewing bright light sources through the pupil and eyelashes [12].

In this paper, we derive various analytical anisotropic reflection models using the scalar Kirchhoff wave theory and the theory of random processes. In particular, we show that the reflected intensity is equal to the spectral density of a simple function $p = e^{i\alpha h}$ of the (random) surface height h. We show that the spectral density can be computed for a large class of surfaces not considered in previous models. We believe that our approach is novel, since the "classic" monographs on scattering from statistical surfaces do not mention such an approach [2, 14].

Diffraction should not be confused with the related phenomenon of *interference*. Interference produces colorful effects due to the phase differences caused by a wave traversing thin media of different indices of refraction, e.g., a soap bubble. Interference effects, unlike diffraction, can be modeled using the ray theory of light alone [7].

To fully understand the derivations in this paper the reader should have a background in Fourier analysis, distribution theory and random processes. Due to a lack of space we refer the reader not versed in these areas to the relevant literature, e.g., [16, 24]. The reader might also want to consult the longer version of this paper available on the CDROM proceedings which contains appendices summarizing the main results from these disciplines. The remainder of this paper is organized as follows. A reader who is interested solely in implementing our new shaders can go directly to Section 6 where the model is stated "as is". Section 2 summarizes the main results from wave theory which are required in this paper. Section 3 presents our derivation. Subsequently, Sections 4 and 5 present several applications of our new reflection model. Section 6 addresses implementation issues and can be read without any advanced mathematical knowledge. Section 7 discusses several results created using our new shaders. Finally, Section 8 concludes, outlining possible directions for future research.

2 Wave Theory and Computer Graphics

In this section we briefly outline some results and concepts from the wave theory necessary to understanding the derivation of our reflection model. We employ the so-called "scalar wave theory of diffraction" [4]. In this approximation the light wave is assumed to be a complex valued scalar disturbance ψ. This theory completely ignores the polarization of light, so its results are therefore restricted to unpolarized light. Fortunately, most common light sources such as the sun and light bulbs are totally unpolarized. The waves generated by these sources also have the property that they fluctuate very rapidly over time. Typical frequencies for such waves are on the order of $10^{14}\ s^{-1}$. In practice this means that we cannot take accurate "snapshots" of a wave. Light waves are thus essentially random and only statistical averages of the wave function have any physical significance. The averaging, denoted by $\langle . \rangle$, can be interpreted either as an average over a long time period or equivalently (via ergodicity) as an ensemble average. An example of a statistical quantity associated with waves is the *irradiance*, $I = \langle |\psi|^2 \rangle$.

We also assume that the waves emanating from the source are stationary. This means that the wave is a superposition of independent monochromatic waves. Consequently, we can restrict our analysis to a wave having a definite wavelength λ associated with it. For visible light, the wavelengths range from the ultraviolet (0.3 microns) to the infrared (0.8 microns) region. Each of these waves satisfies a Helmholtz's wave equation:

$$\nabla^2 \psi + k^2 \psi = 0,$$

where k is the *wavenumber* equal to the reciprocal of the wavelength, $k = 2\pi/\lambda$.

The main task in the theory of diffraction is to solve this wave equation for different geometries. In our case we are interested in computing the reflected waves from various types of surfaces. More precisely, we want to compute the wave ψ_2 equal to the reflection of an incoming planar monochromatic wave $\psi_1 = e^{ik\hat{\mathbf{k}}_1 \cdot \mathbf{x}}$ traveling in the direction $\hat{\mathbf{k}}_1$ from a surface S. Fig. 2 illustrates this situation. The equation relating the reflected field to the incoming field is known as the *Kirchhoff integral*. This equation is a formalization of Huygen's well-known principle that states that if one knows the wavefront at a given moment, the wave at a later time can be deduced by considering each point on the first wave as the source of a new disturbance. This principle implies that once the field on the surface is known, the field everywhere else away from the surface can be computed. The field on the surface is usually related to the incoming field ψ_1 using the *tangent plane* approximation. For a planar surface, the wave theory predicts that a fraction F of the incoming light is specularly reflected. The fraction F is equal to the Fresnel factor for unpolarized light (see p. 48 of [4]). The tangent approximation states that the wave field on the surface is equal to the incoming field plus the field reflected off of the tangent plane at the surface point. Using this relation and the assumption that the "observation point" is sufficiently far removed from the surface, the

Kirchhoff integral is ([2], p. 22):

$$\psi_2 = \frac{ike^{ikR}}{4\pi R}\ (F\mathbf{v} - \mathbf{p}) \cdot \int_S \hat{\mathbf{n}}\ e^{ik\mathbf{v}\cdot\mathbf{s}}\ d\mathbf{s}, \tag{1}$$

where R is the distance from the center of the patch to the receiving point $\mathbf{x}_p$, $\hat{\mathbf{n}}$ is the normal of the surface at $\mathbf{s}$ and the vectors

$$\mathbf{v} = \hat{\mathbf{k}}_1 - \hat{\mathbf{k}}_2 \ \text{ and } \ \mathbf{p} = \hat{\mathbf{k}}_1 + \hat{\mathbf{k}}_2.$$

The vector $\hat{\mathbf{k}}_2$ is equal to the unit vector pointing from the origin of the surface towards the point $\mathbf{x}_p$. To obtain this result it is also assumed that the Fresnel coefficient F is replaced by its average value over the normal distribution of the surface and can thus be taken out of the integral. Eq. 1 is the starting point for our derivation. We will show below that it can be evaluated analytically for a large class of interesting surface profiles. Before we do so, we will also outline how the reflected wave is related to the usual reflection nomenclature used in computer graphics.

In computer graphics, the reflected properties are often modeled using the bidirectional reflection distribution function (BRDF) which is defined as the ratio of the reflected radiance to the incoming irradiance. In this paper we will provide in every case the BRDF corresponding to our reflection model. The relationship between the BRDF and the waves can be shown to be [21]:

$$\text{BRDF} = \lim_{R\to\infty} \frac{R^2}{A\cos\theta_1} \frac{\langle|\psi_2|^2\rangle}{\langle|\psi_1|^2\rangle\cos\theta_2}, \tag{2}$$

where A is the area of the surface and θ_1 and θ_2 are the angles that the vectors $\hat{\mathbf{k}}_1$ and $\hat{\mathbf{k}}_2$ make with the vertical direction (see Fig. 2).

3 Derivation

In this section we demonstrate that the Kirchhoff integral of Eq. 1 can be computed analytically. In this paper, as in related work, we restrict ourselves to the reflection of waves from height fields. We assume that the surface is defined as an elevation over the (x, y) plane. Each surface point is then parameterized by the equation

$$\mathbf{s} \to \mathbf{s}(x, y) = (x, y, h(x, y)), \tag{3}$$

where $h(x, y)$ is a (random) function. The normal to the surface at each point then admits an analytical expression in terms of the partial derivatives h_x and h_y of the height function:

$$\hat{\mathbf{n}}\ d\mathbf{s} \to \hat{\mathbf{n}}(x, y)\ d\mathbf{s} = (-h_x(x, y), -h_y(x, y), 1)\ dxdy.$$

Introducing the notation $\mathbf{v} = (u, v, w)$, it then follows directly that the integral in Eq. 1 acquires the following form:

$$\mathbf{I}(ku, kv) = \int\int (-h_x, -h_y, 1)\, e^{ikwh} e^{ik(ux+vy)}\ dxdy. \tag{4}$$

The integrand can be further simplified by noting that:

$$(-h_x, -h_y, 1)e^{ikwh} = \frac{1}{ikw}(-p_x, -p_y, ikwp),$$

where

$$p(x, y) = e^{ikwh(x,y)}. \tag{5}$$

We now use the common assumption (e.g., [2, 8]) that the integration can be extended over the entire plane. This assumption is usually justified on the grounds that the surface detail is much smaller than the distances over which the surface is viewed. In doing so we observe that the integral of Eq. 4 is now a two-dimensional Fourier transform:

$$\mathbf{I}(ku, kv) = \int\int \frac{1}{ikw}(-p_x, -p_y, ikwp)e^{ik(ux+vy)}dxdy.$$

This important observation can be implemented. Let $P(ku, kv)$ be the Fourier transform of the function p. We observe that differentiation with respect to x (resp. y) in the Fourier domain is equivalent to a multiplication of the Fourier transform by $-iku$ (resp. $-ikv$). This leads to the simple relationship

$$\mathbf{I}(ku, kv) = \frac{1}{w}\ P(ku, kv)\ \mathbf{v}.$$

We have thus related the integral of Eq. 1 directly to the Fourier transform of the function p. Now, since

$$(F\mathbf{v} - \mathbf{p}) \cdot \mathbf{v} = 2F\ (1 - \hat{\mathbf{k}}_1 \cdot \hat{\mathbf{k}}_2),$$

the scattered wave of Eq. 1 is equal to

$$\psi_2 = \frac{ike^{ikR}}{2\pi R} \frac{F(1 - \hat{\mathbf{k}}_1 \cdot \hat{\mathbf{k}}_2)}{w} P(ku, kv). \tag{6}$$

This result shows that the scattered wave field is proportional to the Fourier transform of a simple function of the surface height. Consequently, from Eq. 2, it follows that the BRDF is

$$\text{BRDF} = \frac{k^2F^2G}{4\pi^2Aw^2}\ \langle|P(ku, kv)|^2\rangle, \tag{7}$$

where

$$G = \frac{(1 - \hat{\mathbf{k}}_1 \cdot \hat{\mathbf{k}}_2)^2}{\cos\theta_1\cos\theta_2}. \tag{8}$$

This result and the derivation that leads to it are remarkably simple when compared to derivations that do not employ the Fourier transform, e.g., [2]. More importantly, this treatment is more general, since we have not made any assumptions regarding the function P yet.

We now specialize our results for a homogeneous random function [16]. Homogeneity is a natural assumption since we are interested in the bulk reflection from a large portion of the surface having a certain profile. For example, the portion of the CD depicted in Fig. 1 could have been taken from any part of the CD. However, and this is important, we do not assume that the surface is isotropic. This is mainly where we depart from previous wave physics models in computer graphics. Referring again to Fig. 1 we observe that the CD is clearly not isotropic.

From the definition of the function p (Eq. 5) it follows immediately that this function is also homogeneous. In particular, its correlation function depends only on the separation between two locations:

$$C_p(x', y') = \langle p^*(x, y)p(x + x', y + y')\rangle - |\langle p\rangle|^2,$$

independently of the location (x, y). The Fourier transform of the correlation function is known as the *spectral density* ([16], p. 338):

$$S_p(u, v) = \int\int C_p(x', y')e^{i(ux'+vy')}dx'dy'.$$

The spectral density is a non-negative function which gives the relative contribution of each wavenumber (u, v) to the entire energy. We now show that the average in Eq. 7 is directly related to the spectral density. Indeed, let $\xi = (x, y)$, $\xi' = (x', y')$ and $\zeta = (ku, kv)$, then

$$\langle|P(\zeta)|^2\rangle = \langle P^*(\zeta)P(\zeta)\rangle = \int\!\!\int\langle p^*(\xi)p(\eta)\rangle e^{-i\zeta\cdot\xi}e^{i\zeta\cdot\eta}d\xi d\eta.$$

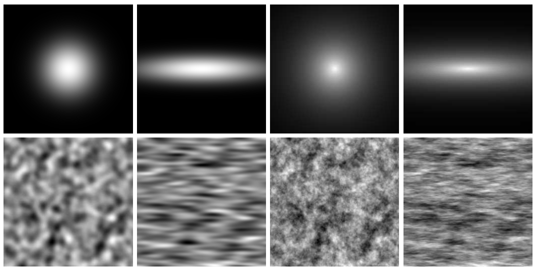

(a) (b) (c) (d)

Figure 3: Effect of the correlation function on the appearance of a random surface. The pictures at the top show plots of different correlation functions with a realization of the corresponding random surface below. The surface types are: (a) isotropic Gaussian, (b) anisotropic Gaussian, (c) isotropic fractal and (d) anisotropic fractal.

With the change of variable $\eta = \xi + \xi'$, this integral becomes

$$\begin{aligned} \iint \langle p^*(\xi) p(\xi + \xi') \rangle e^{i\zeta \cdot \xi'} d\xi d\xi' &= \\ \int d\xi \int (C_p(\xi') + |\langle p \rangle|^2) e^{i\zeta \cdot \xi'} d\xi' &= A\,(S_p(\eta) + 4\pi^2 \delta(\zeta)), \end{aligned}$$

where δ is the two-dimensional Dirac delta function. Consequently, the average in Eq. 7 is a function of the spectral density of the function p:

$$\frac{1}{A} \langle |P(ku, kv)|^2 \rangle = S_p(ku, kv) + 4\pi^2 |\langle p \rangle|^2 \delta(ku, kv).$$

Substituting this result back into Eq. 7 we get:

$$\mathrm{BRDF} = \frac{F^2 G}{w^2} \left(\frac{k^2}{4\pi^2}\, S_p(ku, kv) + |\langle p \rangle|^2 \delta(u, v) \right), \qquad (9)$$

where we have used the fact that $\delta(ku, kv) = \delta(u, v)/k^2$ [24]. Eq. 9 is the main theoretical result of this paper. It shows that the reflection from a random surface is proportional to the spectral density of the random function e^{ikwh}. In the next two sections we apply this result to the derivation of reflection models for various types of surfaces.

4 Anisotropic Rough Surfaces

4.1 General Case

Every surface depicted in Fig. 3 is a realization of a *Gaussian random process*. These processes are entirely defined by their corresponding correlation function depicted in the upper part of Fig. 3. From the figure it is clear that the correlation function determines the general appearance of the random surface. Radially symmetrical correlation functions correspond to isotropic surfaces, c.f., surfaces (a) and (c), while the derivative of the correlation function at the origin also determines smoothness of the surfaces. Consequently, surfaces (a) and (b) are smooth, while surfaces (c) and (d) have a fractal appearance. In this section we further clarify the fact that the reflection from these surfaces is intimately related to the correlation function. Gaussian random processes have the nice property that their characteristic functions admit analytical expressions [2]. These functions are exactly what we require in order to compute the spectral density S_p and the variance $|\langle p \rangle|^2$ appearing in Eq. 9. Indeed, for Gaussian random processes these quantities are related to their surface height counterparts as follows. Firstly, we have the following identities ([16], p. 255):

$$\begin{aligned} \langle p \rangle &= \langle e^{ikwh} \rangle = e^{-g/2} \quad \text{and} & (10) \\ C_p(x, y) &= e^{-g} \left(e^{g C_h(x,y)} - 1 \right), & (11) \end{aligned}$$

where $g = (kw\sigma_h)^2$, and σ_h is the standard deviation of the height fluctuations. Secondly, the spectral density S_p is the Fourier transform of the correlation function C_p ([16], p. 338). To compute this Fourier transform analytically we can use the expansion of the exponential function into an infinite series [2]:

$$e^{g C_h(x,y)} = \sum_{m=0}^{\infty} \frac{g^m}{m!} C_h(x, y)^m.$$

Then using the linearity of the Fourier transform, we can compute the spectral density as

$$S_p = \mathcal{F}\{C_p\} = e^{-g} \sum_{m=1}^{\infty} \frac{g^m}{m!} \mathcal{F}\{(C_h)^m\}. \qquad (12)$$

This requires the computation of the Fourier transform of the surface correlation to a power m. We now give analytical results for the two correlation functions corresponding to the surfaces depicted in Fig. 3. These surfaces are defined by the following two correlation functions:

$$C_1(x, y) = e^{-\frac{x^2}{T_x^2} - \frac{y^2}{T_y^2}} \text{ and } C_2(x, y) = e^{-\sqrt{\frac{x^2}{T_x^2} + \frac{y^2}{T_y^2}}}.$$

In all cases, the *correlation lengths* T_x and T_y control the anisotropy of the surface. Fig. 3.(a) and (b) both correspond to the correlation function C_1. This function is infinitely smooth at the origin, which accounts for the smoothness of the corresponding surfaces. In Fig. 3.(a) $T_x = T_y$ and the surfaces are isotropic. Most previous wave-based models considered only the isotropic case. Fig. 3.(c) and (d) correspond to the correlation function C_2. The corresponding surfaces have a fractal appearance. They are thus good models for very rough materials. In the results section we will see that these surfaces give rise to reflection patterns which are visually different from the smooth case.

For each correlation function, we can compute its Fourier transforms to a power m analytically. They are equal to

$$D_1^m = \frac{\pi T_x T_y}{m} e^{-\frac{U^2 + V^2}{4m}} \text{ and } D_2^m = \frac{2\pi T_x T_y m}{(m^2 + U^2 + V^2)^{3/2}}, \qquad (13)$$

respectively, where $U = kuT_x$ and $V = kvT_y$. By substituting these expressions back into the infinite sum of Eq. 12, we get an analytical expression for the BRDF:

$$\mathrm{BRDF} = \frac{F^2 G}{w^2} e^{-g} \left(\frac{k^2}{4\pi^2} \sum_{m=1}^{\infty} \frac{g^m}{m!} D^m + \delta(u, v) \right), \qquad (14)$$

where D^m is any one of the functions of Eq. 13.

4.2 Discussion

In this section we demonstrate that most previous models in computer graphics are special cases of our new shading model.

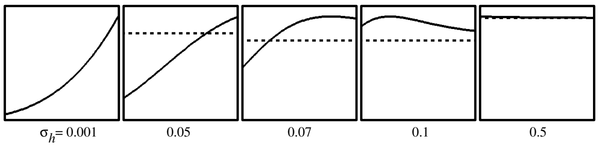

Figure 4: Plots of the BRDF for k ranging from the infrared ($8.06\mu^{-1}$) to the ultraviolet region ($16.53\mu^{-1}$). The reflection is in the specular direction: $\theta_1 = \theta_2 = 45^o$. The plots show the effect of the standard deviation σ_h on the color of the reflection. For low deviations the reflection is bluish, while for higher roughness it tends to flatten out. The dashed line is the geometrical optics approximation.

Born Approximation

When $g << 1$, the infinite sum appearing in Eq. 12 can be truncated to its first term. This is equivalent to the approximation $e^{ikwh} \approx 1 + ikwh$ often taken in physical theories. This approximation should be valid whenever the scales of the surfaces are much smaller than the wavelength of light.

$$\mathrm{BRDF}_{Born} = F^2 G \, e^{-g} \left(\frac{\sigma_h^2 k^4}{4\pi^2} S_h(ku, kv) + \delta(u, v) \right).$$

This result is described in the *Handbook of Optics* [5]. Notice that the BRDF is dependent on the fourth power of the inverse of the wavelength. This means that generally "bluish" light is more strongly scattered than "reddish" light. These surfaces should therefore have a bluish appearance. An interesting feature of this approximation is that one can actually "see" the spectral density of the random surface in its highlight, i.e., any of the plots in Fig. 3 (top).

Geometrical Optics

In the opposite limit when $g >> 1$, an approximate expression for the sum of Eq. 12 can also be derived. This case corresponds to a situation usually encountered in computer graphics when the surface detail is much larger than the wavelength of light. For large g, the Fourier integral only depends on the behavior of the function e^{gC_h} near the origin (see [2, 1] for details):

$$e^{gC_h(x,y)} \approx e^g e^{-g(x^2/T_x^2 + y^2/T_y^2)}.$$

The Fourier transform of this function can be computed analytically and is equal to:

$$S_p(ku, kv) = \frac{\pi T_x T_y}{g} \, e^{-\frac{U^2}{4g}} \, e^{-\frac{V^2}{4g}}.$$

The BRDF in this case is equal to ($e^{-g} \approx 0$):

$$\mathrm{BRDF}_{geom} = \frac{F^2 G}{4\pi w^4 r_x r_y} \, e^{-\frac{u^2}{4w^2 r_x^2}} \, e^{-\frac{v^2}{4w^2 r_y^2}}, \qquad (15)$$

where $r_x = \sigma_h / T_x$ and $r_y = \sigma_h / T_y$. This distribution is a generalization of the isotropic distributions found in the Blinn and Cook-Torrance models where there is only one roughness parameter "m". In fact, our model closely resembles Ward's anisotropic reflection model [22]. As in the Cook-Torrance model, BRDF_{geom} is only dependent on the wavelength of light through the Fresnel factor F, as there is no other explicit dependence on wavelength: k does not explicitly appear in the distribution.

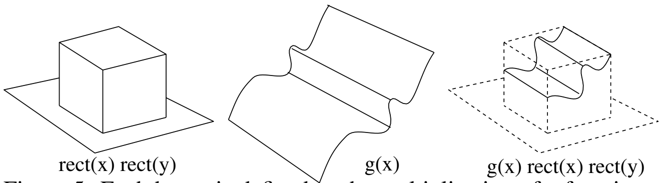

Figure 5: Each bump is defined as the multiplication of a function $g(x, y)$ with the product of box-like functions.

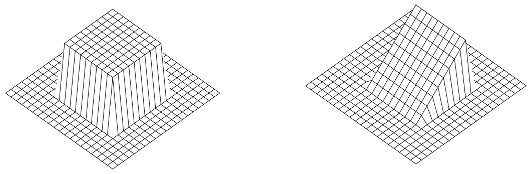

Figure 6: Two different bump functions: (1) constant, (2) linear in one coordinate.

Isotropic Distributions

The He-Torrance [8] and the Nayar [13] reflection models are obtained when our model is restricted to the class of isotropic surfaces corresponding to Fig. 3.(a). Using our result for the correlation function C_1 with $T_x = T_y$, we essentially recover both of these models. It is worth noting that one of the versions of the He-Torrance model handles polarization effects while our model doesn't. This is because they used the vector valued version of the Kirchhoff integral. However, in practice it seems He-Torrance have only used their unpolarized version to create the pictures accompanying their paper. The dependence on wavelength (as in our model) is a function of the Fresnel factor F and the function $k^2 \; S_p(ku, kv)$. In Fig. 4 we illustrate the dependence of this function on wavenumber k for different surface deviations σ_h. The reflection goes from a k^2 dependence to a flat spectrum. Notice that in the midrange we actually get a small yellowish hue. The figure also demonstrates that for $\sigma_h > 0.5$ the geometrical optics model, shown as a dashed line, is a very good approximation. In practice we have found that whenever $g > 10$ the pictures generated with the geometrical optics approximation are visually indistinguishable from pictures generated using the exact model.

5 Diffraction from Periodic-like Surfaces

We now turn to an application that most clearly demonstrates the power of our new reflection model.

Many surfaces have a micro-structure that is made out of similar "bumps". A good example is a compact disk which has small bumps that encode the information distributed over each "track". Fig. 1 is a magnified view of the actual surface of a compact disk. Notice in particular that the distribution of bumps is random along each track but that the tracks are evenly spaced. In this section we derive general formulae for certain shapes of bumps, and then specialize the results for a CD-shader.

symbol	description	size
h_0	height of a bump	0.15 μm
a	width of a bump	0.5 μm
b	length of a bump	1 μm
Δx	separation between the tracks	2.5 μm
ν_y	density of bumps on each track	0.5 $(\mu m)^{-1}$

Table 1: Typical dimensions of a compact disk.

We assume that the surface is given by a superposition of bumps:

$$h(x,y)=\sum_{n=-\infty}^{\infty}\sum_{m=-\infty}^{\infty} b(x-x_n,y-y_m), \tag{16}$$

where the locations (x_n, y_m) are assumed to be either regularly spaced or randomly (Poisson) distributed. To handle the two cases simultaneously, we assume that x_n is evenly spaced and that y_n is Poisson distributed. Extensions to the case where both locations are evenly spaced or where both are Poisson distributed should be obvious from our results. Let Δx be the constant spacing between the x-locations: $x_n = n\Delta x$. The random Poisson distribution of the locations y_m is entirely specified by a density ν_y of bumps per unit length. The function $b(x, y)$ appearing in Eq. 16 is a "bump function": a function with (small) finite support. We will assume that the bump function has the following simple form:

$$b(x,y)=h_0\ g(x/a)\mathrm{rect}(x/a)\mathrm{rect}(y/b), \tag{17}$$

where a, b and h_0 define the width, length and height of each bump respectively ($a \le \Delta x$). Typical values of these parameters for a CD are provided in Table 1. The function rect equals one on the interval $[-1/2, 1/2]$ and zero elsewhere. Fig. 5 illustrates our definition of a bump. Our derivation is valid for arbitrary g, however, we provide an analytical expression only for the following two functions:

$$g^0(x)=1 \quad \text{and} \quad g^1(x)=1/2+x. \tag{18}$$

The bumps corresponding to these functions are depicted in Fig. 6. The function g^0 is a good approximation of the bumps found on a CD and the function g^1 can be used to model diffraction gratings.

The function $p(x, y)$ defined by Eq. 5 in our case is equal to:

$$p(x,y)=\sum_{n=-\infty}^{\infty}\sum_{m=-\infty}^{\infty}\phi((x-x_n)/a,(y-y_m)/b), \tag{19}$$

where $\phi(x,y) = e^{i\alpha g(x)}\mathrm{rect}(x)\mathrm{rect}(y)$ and $\alpha = kwh_0$. We dropped a constant term "1" that accounts for the space between the bumps and only adds a delta spike in the specular direction.

A simple computation shows that the Fourier transform of the function $p(x, y)$ is equal to

$$P(u,v)=\sigma_x(u)\sigma_y(v)\ ab\ \Phi(au,bv),$$

where $\Phi(u, v)$ is the Fourier transform of $\phi(x, y)$ and

$$\sigma_x(u)=\sum_{n=-\infty}^{\infty} e^{iun\Delta x} \quad \text{and} \quad \sigma_y(v)=\sum_{m=-\infty}^{\infty} e^{ivy_m}. \tag{20}$$

To compute the spectral density of Eq. 9 we note that:

$$S_p(u,v)=(ab)^2|\Phi(au,bv)|\ |\sigma_x(u)|^2\ S_{\sigma_y}(v).$$

The spectral density and the average of the sum of random Poisson distributed locations are both equal to the density ν_y (see [16] p. 561):

$$S_{\sigma_y}(v)=\nu_y \quad \text{and} \quad \langle\sigma_y\rangle=\nu_y.$$

The sum of evenly spaced location x_n is a bit harder to deal with. First we need the following two results from the theory of distributions (see pp. 54-55 of reference [24]):

$$\sum_{n=-\infty}^{\infty} e^{iun}=2\pi\sum_{n=-\infty}^{\infty}\delta(u-2\pi n) \quad \text{and} \quad \delta(sz+t)=\frac{1}{s}\delta(z+t/s),$$

where $s > 0$ and t are real numbers. The first of these two equalities is known as "Poisson's summation formula". Using these results we can express the square of the sum σ_x in terms of delta distributions only:

$$|\sigma_x(u)|^2=\frac{(2\pi)^2}{\Delta x^2}\sum_{n=-\infty}^{\infty}\delta(u-2\pi n/\Delta x).$$

We can now compute the spectral density S_p by putting all these computations together:

$$S_p(ku,kv)=b^2\nu_y\lambda\sum_{n=-\infty}^{\infty}|\Phi_n(kv)|^2\delta(u-n\lambda/\Delta x), \tag{21}$$

where

$$|\Phi_n(kv)|^2=\frac{a^2}{\Delta x^2}|\Phi(2\pi na/\Delta x,kv)|^2. \tag{22}$$

The function $|\Phi|^2$ can be computed analytically for the two bumps depicted in Fig. 6:

$$\begin{aligned}|\Phi^0(au,bv)|^2 &= 2(1-\cos(\alpha))\mathrm{sinc}^2(au/2)\mathrm{sinc}^2(bv/2), && (23)\\ |\Phi^1(au,bv)|^2 &= \big(\mathrm{sinc}^2(\alpha_0/2)-2\mathrm{sinc}(\alpha_0/2)\times \\ &\quad \mathrm{sinc}(au/2)\cos(\alpha/2)+\mathrm{sinc}^2(au/2)\big)\,\mathrm{sinc}^2(bv/2), && (24)\end{aligned}$$

where $\alpha_0 = \alpha + au$. Putting all these pieces together we get the following expression for the BRDF:

$$\mathrm{BRDF}=\frac{F^2G}{w^2}b^2\nu_y\sum_{n=-\infty}^{\infty}|\Phi_n(kv)|^2\delta(u-n\lambda/\Delta x)(k+\nu_y\delta(u)).$$

6 Implementation

We have implemented our reflection models as various shaders in our MAYA animation system. Any model created in that package can be rendered using our new shaders. The fact that our shaders have been included in a commercial product should be a sufficient proof of their practicality.

As in [9], we model the anisotropy of the surface by assigning an orthonormal frame at each point of the surface. In the case of a parametric surface, the most natural choice for this frame is to take the normal and the two vectors tangent to the iso-parameter lines. We have also added an additional rotation angle to the frame around the normal. When this angle is texture mapped, it allows us to create effects such as brushed metal (Fig. 8.(a)).

The general form of our shader is

$$\mathrm{BRDF}=|F(\theta_1')|^2\ G(\mathbf{k}_1,\mathbf{k}_2)\ S(\mathbf{k}_1,\mathbf{k}_2)\ \left(D(\mathbf{v},\lambda)+r\mathrm{Env}\right),$$

where F is the Fresnel factor [6], S is a shadowing function [8], G is a geometrical factor defined by Eq. 8 in Section 3 and D is a distribution function that is related to the micro-geometry of the surface. The function "Env" returns the color in the mirror direction of $\mathbf{k}_2$ from an environment map and the factor r accounts for how much the surface reflects direct illumination. The vector $\mathbf{v} = (u, v, w)$ is the angle midway between $-\mathbf{k}_1$ and $\mathbf{k}_2$. The Fresnel factor is evaluated at the angle θ_1' that the direction $\mathbf{k}_1$ makes with the vector $\mathbf{v}$. The Fresnel factor varies with the index of refraction of the metallic surface and is wavelength dependent [6]. We do not use the He-Torrance shadowing function since it is restricted to isotropic surfaces. Instead, we employ a model introduced by Sancer [18]. For convenience, we have included this model in Appendix A. The distribution D is the most important component of our model and is now described in more detail.

In the previous sections we have derived distribution functions for both the random surfaces depicted in Fig. 3 and for periodic-like profiles such as the one shown in Fig. 1. When the surface is random, the distribution is defined by the three parameters σ_h, T_x and T_y. The variance σ_h^2 models the average height fluctuations of the surface and the parameters T_x and T_y model the amount of correlation of the micro-surface in the directions of the local frame. See Section 3 for further details on these quantities. When $T_x = T_y$, the surface is isotropic. In the most general case, the distribution D is computed by the infinite sum appearing in Eq. 14. In Appendix B, we provide a stable implementation of this sum. As pointed out in Section 4.2, the sum is very well approximated by the geometrical optics approximation of Eq. 15, when $g = (kw\sigma_h)^2$ is large (see also Fig. 4). The factor "r" is equal to $\exp(-g)$. The smoother the surface, the more indirect illumination is directly reflected off of it.

The implementation of periodic-like profiles giving rise to colorful diffraction patterns is different. When evaluating the distribution D, the values u and v (and w) are determined by the incoming and outgoing angles. The incoming light is usually assumed to be an incoherent sum of many monochromatic waves whose number is proportional to the distribution $L(\lambda)$ of the light source. To determine the intensity and the color of the light reflected in the outgoing direction, we first compute the wavelengths λ_n for which $L(\lambda)$ is non zero and for which the delta spikes in Eq. 21 are non-zero. This only occurs when $\lambda_n = \Delta x u/n$ and $n \neq 0$. When $n = 0$, all wavelengths contribute intensities in the specular direction $u = 0$. In general, visible light is comprised only of waves with wavelengths between $\lambda_{min} = 0.4\mu m$ and $\lambda_{max} = 0.7\mu m$. This means that the indices n are constrained to lie in the range $\Delta x u[1/\lambda_{max}, 1/\lambda_{min}]$ if $u > 0$ and in the range $\Delta x u[1/\lambda_{min}, 1/\lambda_{max}]$ when $u < 0$. Once these wavelengths are determined, the red, green and blue components of the distribution D are computed as follows

$$D_{rgb} = b^2 \nu_y \sum_{n=N_{min}}^{N_{max}} \frac{1}{\lambda_n} \mathrm{Spec}_{rgb}(\lambda_n) L(\lambda_n) \left| \Phi_n \left(\frac{2\pi v}{\lambda_n} \right) \right|^2,$$

where Spec_{rgb} is a function that for each wavelength returns the corresponding color. This function can either be constructed from psychophysical experiments or simply set by an animator as a "ramp". In our implementation we constructed a ramp function from standard RGB response curves. See Eq. 22 for a definition of the function Φ_n.

7 Results

Once the shaders were implemented in MAYA, it was an easy task to generate results demonstrating the power of our new shading model. In Fig. 7 we show the effect of some of the parameters of our model on the appearance of the surfaces. In each rendering we chose to have a spectrally flat Fresnel factor to demonstrate the dependence of the distribution on wavelength. For the Gaussian correlations the reflection is more bluish for small roughness and becomes whiter for larger roughness, in accordance with the analysis of Section 4.2. The reflection from fractal surfaces is quite interesting: bluish for small roughness, then yellowish for intermediate roughness and finally white for large roughness. The third row of spheres exhibits the effect of the separation and twist angle parameters of our diffraction shader. We used a different texture map for the twist angle of each one of the three "diffraction cones" at the bottom of Fig. 7.

Fig. 8 shows several renderings created in this manner. In each case we have texture mapped the directions of anisotropy to add more interesting visual detail. Fig. 8.(a) demonstrates that this can be employed to create a "brushed metal" look. In Fig. 8.(b) we textured both the roughness and the degree of anisotropy of the surface. Fig. 8.(c) is a picture of a CD illuminated by a directional light source. Notice that all the highlights appear automatically in the correct places when the data from Table 1 is used. Fig. 8.(d) is an example of the use of our diffraction grating model. Notice all the subtle coloring effects that result (especially when viewing the corresponding animation). These colorful effects would be hard to model by trial and error without properly modeling the wave properties of light.

The effects of the anisotropy and of diffraction are most pronounced in an animation when moving either the object or the light sources. For this reason we have included some animations on the CDROM proceedings.

8 Conclusions

In this paper we have proposed a new class of reflection models that take into account the wave-like properties of light. For the first time in computer graphics, we have derived reflection models that properly simulate the effects of diffraction. We have shown that our models can be easily implemented as standard shaders in our MAYA animation software. Our derivations, while mathematically involved, are simpler and more general than previously published results in this area. In particular, our use of the Fourier transform has proven to be a very powerful tool in deriving new reflection models.

In future work, we hope to extend our model to an even wider class of surfaces by relaxing some of the assumptions in our model. Presently, our model only accounts for the reflection from metallic surfaces and ignores multiple-scattering. It would be interesting to derive more general models that take into account subsurface scattering by waves. It seems unlikely that the effects of multiple scattering might be captured by an analytical model. An alternative would be to fit analytical models to either the results from a Monte-Carlo wave simulation or to experimentally measured data.

As well, we wish to extend our work to the computation of the fluctuations of the intensity field [10]. In this manner we can compute exact texture maps for given surface profiles. We could achieve this by deriving analytical expressions for the higher order statistics of the reflected intensity field. More specifically, we hope to extend our previous work on stochastic rendering of density fields to surfaces [19].

Acknowledgments

Thanks to Duncan Brinsmead for suggesting the "twist angle", for helping me write the MAYA plugin and for creating Figs. 8.(a) and (b). Thanks to Greg Ward for encouraging me to study the wave theory and for commenting on the first draft of this paper. Thanks also to Pamela Jackson for proofreading the paper.

A A Shadowing Function

The shadowing function used in He's model applies only to isotropic surfaces. For this reason we have used a different model derived by Sancer [18]. The shadowing function is valid for a Gaussian random surface having a correlation function C_h and standard deviation σ_h:

$$S = \begin{cases} (C_1+1)^{-1} & \text{if } u = v = 0 \text{ and } \theta_1 \le \theta_2 \\ (C_2+1)^{-1} & \text{if } u = v = 0 \text{ and } \theta_2 \le \theta_1 \\ (C_1+C_2+1)^{-1} & \text{else} \end{cases},$$

where

$$C_i = \sqrt{\frac{2|\beta_i|}{\pi}} \tan\theta_i \exp\left(-\frac{\cot^2\theta_i}{2|\beta_i|}\right) - \mathrm{erfc}\left(\frac{\cot\theta_i}{\sqrt{2|\beta_i|}}\right)$$

$$\beta_i = \sigma_h^2 \left(C_{h,xx}\cos^2\phi_i + C_{h,xy}\sin 2\phi_i + C_{h,yy}\sin^2\phi_i\right),$$

where $i = 1, 2$ and $C_{h,xx}$ is the second derivative with respect to x of the correlation function at the origin. Since the derivatives of the correlation function depend on the correlation lengths T_x and T_y, this clearly shows that this shadowing function takes into account the anisotropy of the surface.

B Computing Infinite Sums

The following piece of code will compute the distribution of reflected light from the surface:

```
compute_D (lambda,u,v,w,s_h,Tx,Ty)
  k = 2*PI/lambda;
  g = k*s_h*w; g *= g;
  if ( g>10 )
    return D_geom(u,v,w,s_h/Tx,s_h/Ty);
  tmp=1; sum=log_g=0;
  for(m=1;abs(tmp)>EPS||m<3*g;m++) {
    log_g += log(g/m); tmp = exp(log_g-g);
    sum += tmp*D(m,k*u,k*v,Tx,Ty);
  }
  return lambda*lambda*sum
```

The function `D()` is any one of the functions of Equation 13. This routine is a stable implementation of the infinite sum appearing in Equation 14. A naive implementation of the sum results in numerical overflows. The condition "`m<3*g`" is there to make sure that we do not exit the loop too early. This is an heuristic which has worked well in practice.

References

[1] E. Bahar and S. Chakrabarti. Full-Wave Theory Applied to Computer-Aided Graphics for 3D Objects. *IEEE Computer Graphics and Applications*, 7(7):46–60, July 1987.

[2] P. Beckmann and A. Spizzichino. *The Scattering of Electromagnetic Waves from Rough Surfaces*. Pergamon, New York, 1963.

[3] J. F. Blinn. Models of Light Reflection for Computer Synthesized Pictures. *ACM Computer Graphics (SIGGRAPH '77)*, 11(3):192–198, August 1977.

[4] M. Born and E. Wolf. *Principles of Optics. Sixth (corrected) Edition*. Cambridge University Press, Cambridge, U.K., 1997.

[5] E. L. Church and P. Z. Takacs. *Chapter 7. Surface Scattering.* In *Handbook of Optics (Second Edition). Volume I: Fundamentals, Techniques and Design*. McGraw Hill, New York, 1995.

[6] R. L. Cook and K. E. Torrance. A Reflectance Model for Computer Graphics. *ACM Computer Graphics (SIGGRAPH '81)*, 15(3):307–316, August 1981.

[7] J. S. Gondek, G. W. Meyer, and J. G. Newman. Wavelength dependent reflectance functions. In *Computer Graphics Proceedings, Annual Conference Series, 1993*, pages 213–220, 1994.

[8] X. D. He, K. E. Torrance, F. X. Sillion, and D. P. Greenberg. A Comprehensive Physical Model for Light Reflection. *ACM Computer Graphics (SIGGRAPH '91)*, 25(4):175–186, July 1991.

[9] J. T. Kajiya. Anisotropic Reflection Models. *ACM Computer Graphics (SIGGRAPH '85)*, 19(3):15–21, July 1985.

[10] W. Krueger. Intensity Fluctuations and Natural Texturing. *ACM Computer Graphics (SIGGRAPH '88)*, 22(4):213–220, August 1988.

[11] H. P. Moravec. 3-D Graphics and the Wave Theory. *ACM Computer Graphics (SIGGRAPH '81)*, 15(3):289–296, August 1981.

[12] E. Nakamae, K. Kaneda, and T. Nishita. A Lighting Model Aiming at Drive Simulators. *ACM Computer Graphics (SIGGRAPH '90)*, 24(4):395–404, August 1990.

[13] S. K. Nayar, K. Ikeuchi, and T. Kanade. Surface Reflection: Physical and Geometrical Perspectives. *IEEE Transactions on Pattern Analysis and Machine Intelligence*, 13(7):611–634, July 1991.

[14] J. A. Ogilvy. *Theory of Scattering from Random Rough Surfaces*. Adam Hilger, Bristol, U.K., 1991.

[15] Tomohiro Ohira. A Shading Model for Anisotropic Reflection. *Technical Report of The Institute of Electronic and Communication Engineers of Japan*, 82(235):47–54, 1983.

[16] A. Papoulis. *Probability, Random Variables, and Stochastic Processes*. McGraw-Hill, Systems Science Series, New York, 1965.

[17] P. Poulin and A. Fournier. A Model for Anisotropic Reflection. *ACM Computer Graphics (SIGGRAPH '90)*, 24(4):273–282, August 1990.

[18] M. I. Sancer. Shadow Corrected Electromagnetic Scattering from Randomly Rough Surfaces. *IEEE Transactions on Antennas and Propagation*, AP-17(5):577–585, September 1969.

[19] J. Stam. Stochastic Rendering of Density Fields. In *Proceedings of Graphics Interface '94*, pages 51–58, Banff, Alberta, May 1994.

[20] D. C. Tannenbaum, P. Tannenbaum, and M. J. Wozny. Polarization and Birefringency Considerations in Rendering. In *Computer Graphics Proceedings, Annual Conference Series, 1994*, pages 221–222, July 1994.

[21] K. Tomiyasu. Relationship Between and Measurement of Differential Scattering Coefficient (σ^0) and Bidirectional Reflectance Distribution Function (BRDF). *SPIE Proceedings. Wave Propagation and Scattering in Varied Media*, 927:43–46, 1988.

[22] G. J. Ward. Measuring and Modelling Anisotropic Reflection. *ACM Computer Graphics (SIGGRAPH'92)*, 26(2):265–272, July 1992.

[23] E. Wolf. Coherence and Radiometry. *Journal of the Optical Society of America*, 68(1), January 1978.

[24] A. H. Zemanian. *Distribution Theory and Transform Analysis: An Introduction to Generalized Functions, with Applications*. Dover, New York, 1987.

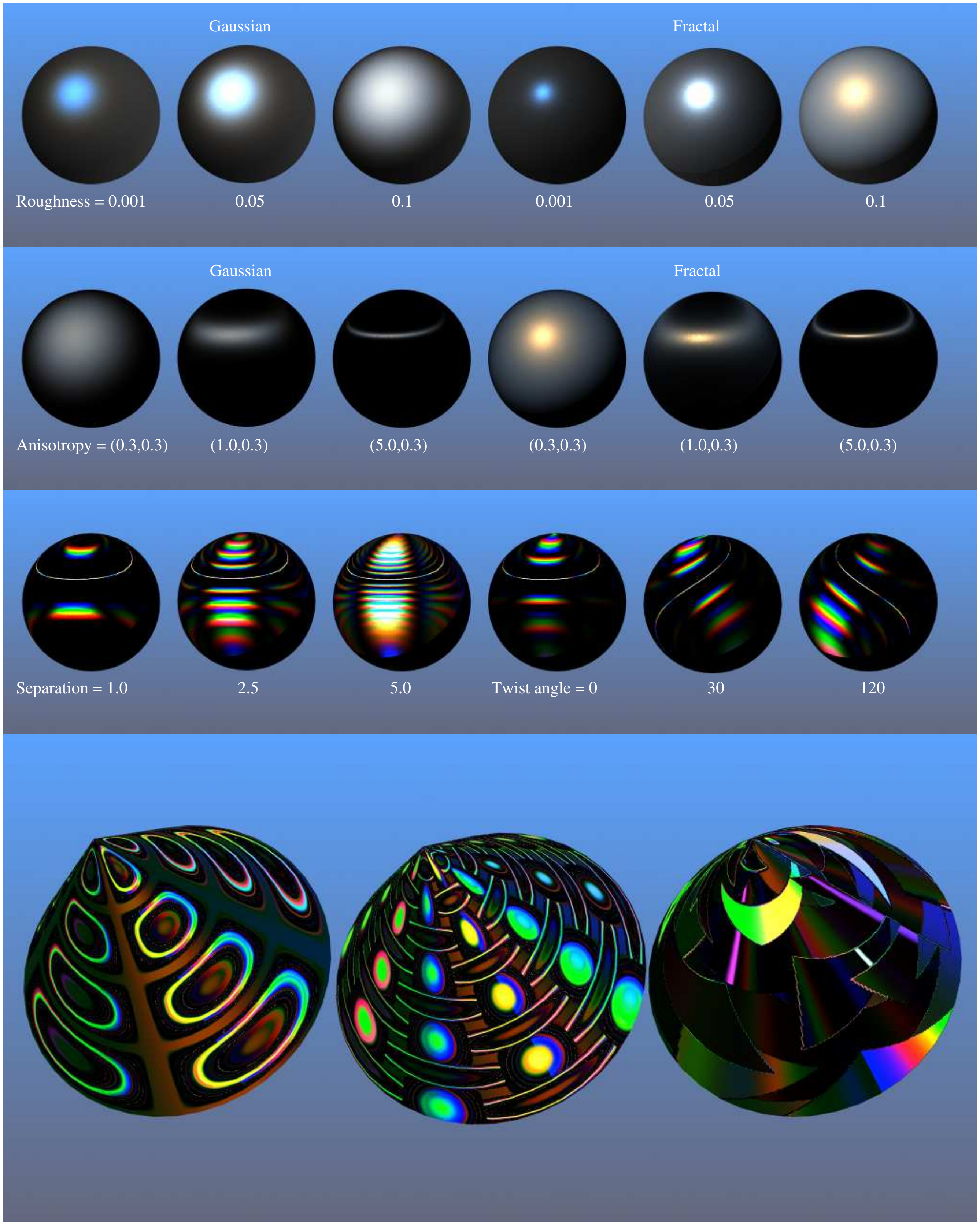

Figure 7: Effect of some of the parameters.

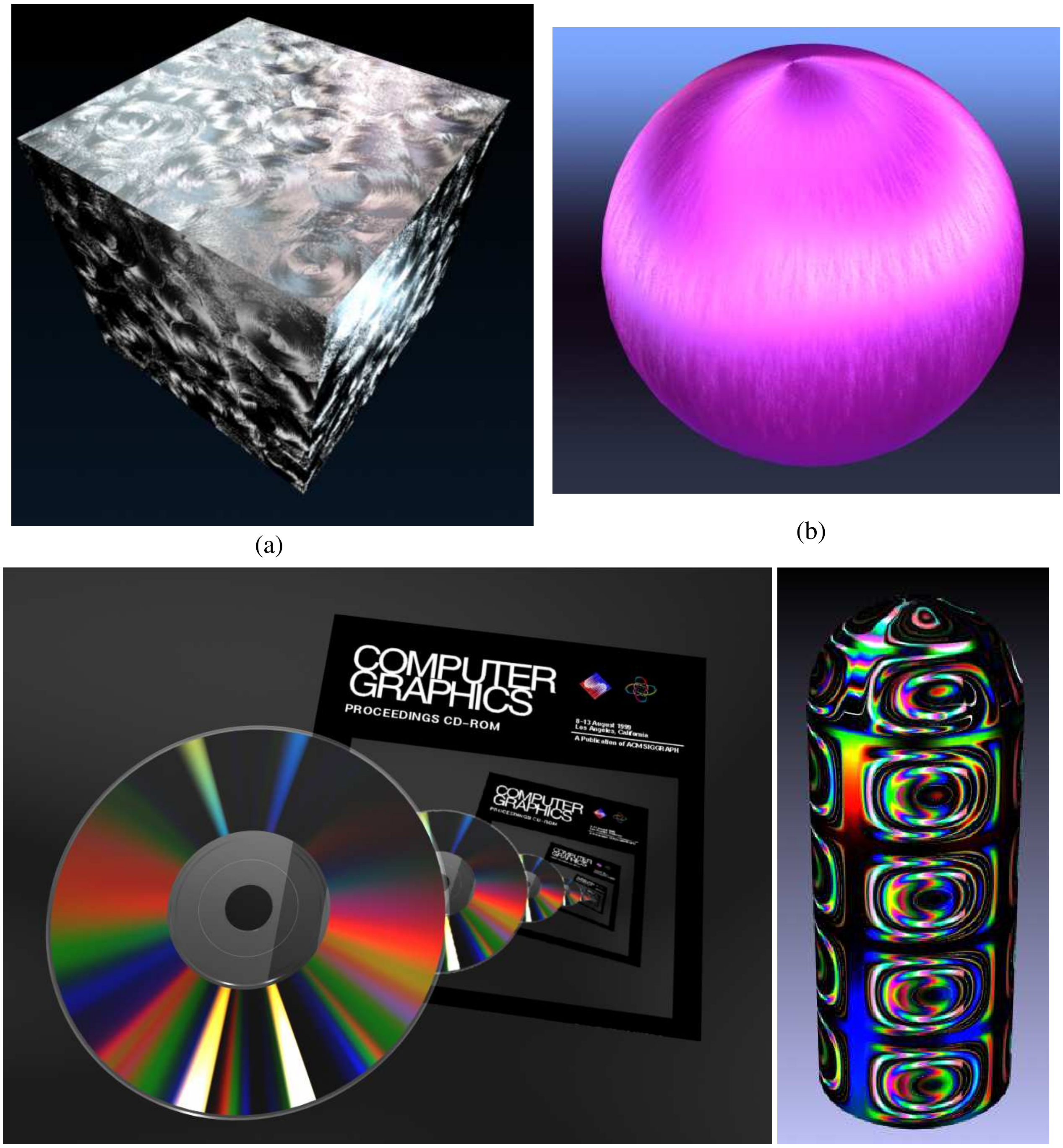

(a) (b)

(c) (d)

Figure 8: More pictures.